Dual-Polarized WDM Access Network With Fiber to the Extension (FTTE) Connection

Chien-Hung Yeh [ID], Wei-Hung Hsu [ID], Bo-Yin Wang [ID], Jhao-Ren Chen [ID], Wei-Yao You [ID], and Chi-Wai Chow

Abstract—In this study, a symmetric polarization-division-multiplexing (PDM) wavelength-division-multiplexing passive optical network (WDM-PON) with fiber to the extension (FTTE) architecture is presented and investigated. The proposed PON can also avoid the Rayleigh backscattering (RB) interference noise. Here, each WDM wavelength can produce 25 Gbit/s on-off keying (OOK) and 10 Gbit/s OOK modulation channels simultaneously in x- and y-polarizations (Pol_x and Pol_y) through PDM method for 25 and 105 km single-mode fiber (SMF) transmissions without dispersion compensation. The measured minimal power budget of 25 and 10 Gbit/s downstream and upstream signals are 29 and 35.1 dB and 29.8 and 31.5 dB, respectively, at the forward error correction (FEC) target. Therefore, the proposed PDM WDM-PON architecture can not only offer symmetric 35 Gbit/s downstream and upstream connections by the dual-polarized wavelength, but also can avoid the RB-induced interference noise. In addition, the presented dual-polarized downstream signal also can provide information security in physical layer, when the unauthorized user occupies unlawfully.

Index Terms—Polarization-division-multiplexing (PDM), WDM-PON, Fiber to the extension (FTTE), Rayleigh backscattering (RB).

I. INTRODUCTION

RECENTLY, due to the immediate requirements of artificial intelligence (AI), 5G mobile, cloud computing, big data, internet, 4 K/8 K video service, and video conferencing for end user, developing the time-division-multiplexing (TDM) and wavelength-division-multiplexing (WDM) passive optical networks (PONs) have been proposed and studied to meet the desire in last mile access [1]–[4]. The PON access have the advantages of high flexibility, wide capacity, and cost-effectiveness [5]. Several PON networks have been presented to deliver the downstream traffic from 1 to 40 Gbit/s. To achieve 40 Gbit/s downstream rate, the time- and wavelength-division-multiplexing (TWDM) PON has been demonstrated [6], [7]. Hence, each optical network unit (ONU) of TWDM-PON could offer the

traffic rate of >10 Gbit/s downstream and 2.5 Gbit/s upstream [8]. Furthermore, to increase the data rates for customer, using hybrid polarization-division-multiplexing (PDM), WDM and optical coherent technologies in PON networks for delivering point to point (PtP) traffic data have also been investigated [9]–[13]. The PDM method could double data rate of each WDM wavelength based on orthogonal dual-polarized channel [14], [15]. Comparison of the TWDM-PONs (ITU-T G.989 or IEEE GE-PON) with data-sharing access, the WDM-PONs could provide >10 Gbit/s modulation rate to each ONU by PtP connection. Thus, the multiple WDM laser sources are required in the central office (CO) and each ONU modules. To minimize deployment costs, use of the same wavelengths for downstream and upstream connections would be the first consideration in WDM access. However, this way also could cause the RB-induced noise in such network.

While the same wavelengths are applied for downstream and upstream connections in the WDM-PON systems simultaneously, the RB-induced noise could be produced at the optical receiver (Rx) in the central office (CO) and the ONU [16], [17]. Moreover, with the increase of fiber transmission length increasingly, the RB-induced noise could be significant [18]. To mitigate the RB noise in WDM access network, several methods have been proposed, such as using the separating dual-band WDM wavelengths, electrical filtering effect, wavelength-shifted modulation, and special fiber network architecture [19]–[23].

In this paper, we present and demonstrate a symmetric PDM WDM-PON architecture with fiber to the extension (FTTE) connection for long-reach fiber transmission. Based on the output feature of $2 \times N$ WDM multiplexer in the presented PON network, the RB induced beat noise can also be mitigated. According to the PDM property, each WDM wavelength can be divided two orthogonal polarization (Pol_x and Pol_y) channels to carry 25 and 10 Gbit/s on-off keying (OOK) downstream traffic for 25 and 105 km single-mode fiber (SMF) transmissions, respectively, without any dispersion compensation. Besides, the upstream traffic also utilizes the symmetric 25 and 10 Gbit/s modulation for data link. To understand the bit error rate (BER) performance of downstream and upstream signals, the wavelengths of λ_1 to λ_4 and λ_2 to λ_5 with dual-polarized channel are applied for measurement, respectively. Based on the obtained results, the minimal power budget of 25 and 10 Gbit/s downstream and upstream wavelengths with Pol_x- and Pol_y-channels are 29 and 35.1 dB and 29.8 and 31.5 dB, respectively, under the FEC threshold. Moreover, the downstream wavelength can cause jamming sequence to secure the downstream information due to the two combined 25 and 10 Gbit/s signals,

Chien-Hung Yeh, Wei-Hung Hsu, Bo-Yin Wang, Jhao-Ren Chen, and Wei-Yao You are with the Department of Photonics, Feng Chia University, Taichung 40724, Taiwan (e-mail: yeh1974@gmail.com; whhsu@fcu.edu.tw; paul19961103@icloud.com; denny92010@gmail.com; jeter110608@gmail.com).

Chi-Wai Chow is with the Department of Photonics, College of Electrical and Computer Engineering, National Chiao Tung University, Hsinchu 30010, Taiwan (e-mail: cwchow@faculty.nctu.edu.tw).
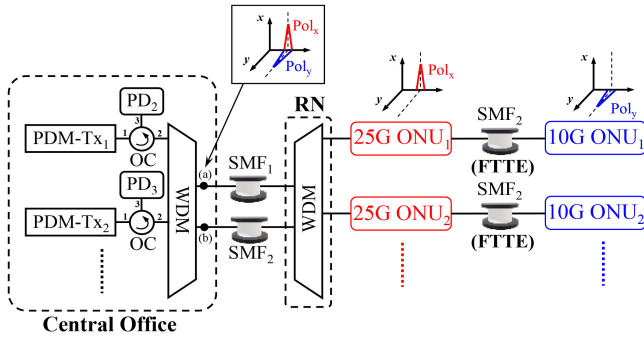
Fig. 1. Proposed PDM WDM-PON architecture with the FTTE connection for short-reach and long-reach fiber transmission.

when the unauthorized user occupied unlawfully. As a result, the presented PDM WDM-PON architecture not only offer symmetric 35 Gbit/s downstream and upstream transmissions by dual-polarized wavelength, but also mitigate the RB noise and cause the data security and protection for end user.

II. EXPERIMENT AND RESULTS

To increase the data efficiency of WDM wavelength, integrating the polarization-division-multiplexing (PMD) technique in WDM-PON access would be alternative solution. Fig. 1 exhibits the proposed PMD WDM access with fiber to the extension (FTTE) architecture for long reach fiber transmission. As seen in Fig. 1, each WDM downstream wavelength (λ_1 to λ_N) can be divided two orthogonal polarization channels. Hence, the orthogonal x- and y-polarization (Pol_x and Pol_y) channels could carry two different modulation rates for different capacity applications to end user in the central office (CO). Then, the WDM downstream wavelengths could be integrated by $2 \times N$ WDM multiplexer and then transmitted through the output port "a", as illustrated in Fig. 1. Next, through a length of single-mode fiber (SMF_1), the WDM wavelengths could be separated by $2 \times N$ WDM demultiplexer at the remote node (RN). Next, each WDM wavelength with two orthogonal dual-polarized signals could apply 25 and 10 Gbit/s modulation rates and launch into the 25G ONU and 10G ONU for receiving the Pol_x- and Pol_y-based downstream traffic, respectively, as shown in Fig. 1. The 10 Gbit/s Pol_y-based downstream would be delivered by the FTTE architecture to the 10G ONU through a length of SMF_2 long-reach transmission. Moreover, to decode the corresponding Pol_x- and Pol_y-based modulation signals in the access system, we could utilize the x-and y-direction polarizer (POL_x and POL_y) in the 25G and 10G ONUs for matching, respectively. As a result, each WDM downstream wavelength could provide two different modulation traffics simultaneously for short-reach 25G ONU and long-reach 10G ONU in the proposed PON based on dual-polarized wavelength without any dispersion compensation.

In the demonstration, due to the WDM downstream wavelength with two dual-polarized modulation traffic, the 25G and 10G ONUs could receive the two modulated rates simultaneously. If the downstream wavelength is attacking and occupying by the unauthorized user, the blended modulation signal would

not be decoded due to the signal interference of two blended 25 and 10 Gbit/s channels. Therefore, the proposed dual-polarized WDM downstream configuration would also produce the data security in physical layer. We require to exploit the POL_x and POL_y in the 25G and 10G ONUs, respectively, to permit the corresponding polarization signal for avoiding signal interference.

As we know, the $2 \times N$ WDM multiplexer has a periodic wavelength output arrangement, as exhibited in Fig. 2(a). Here, the connected port "a" only allow the wavelengths of λ_1 to λ_N to deliver each channel at corresponding output port. And the wavelengths of λ_2 to λ_{N+1} could enter the port "b" for transporting. In the presentation, we can apply the wavelengths of λ_1 to λ_N and λ_2 to λ_{N+1} regarding as the downstream and upstream signals, respectively, through the connected port "a" and "b" of $2 \times N$ WDM multiplexer. Moreover, once the wavelengths of downstream and upstream are the same in WDM-PON for data access simultaneously, the RB-induced signal noise would be cause at the optical Rx in the CO and ONU [17]. The schematic of RB-induced noises of downstream and upstream ($RB_{\lambda 1}$ and $RB_{\lambda 2}$) in the presented WDM-PON system are illustrated in Fig. 2(b). Hence, when the downstream and upstream wavelengths with a frequency spacing of Δf are used in the presented PON for bidirectional connection, the RB interferometric beat noise could be avoided.

Fig. 3 presents the experimental setup of proposed PDM WDM-PON architecture with long-reach FTTE application for proof of concept. First, we execute the signal performance of dual-polarized downstream transmission. To demonstrate and generate the different WDM downstream wavelength, a tunable laser source (TLS) is used in the CO for tuning. Here, we select four WDM wavelengths which represent the 1540.16 (λ_1), 1540.95 (λ_2), 1541.75 (λ_3), and 1542.54 nm (λ_4), respectively, serving as the downstream channels. As seen in Fig. 2, the downstream wavelength can be separated two signals by a 1×2 and 50:50 optical coupler (CPR) and connected to the two polarization controllers (PCs), a 40 GHz Mach-Zehnder modulator (MZM_1) and a 10 GHz Mach-Zehnder modulator (MZM_2) in the upper and lower fibers. Then, the two wavelengths pass through a polarization beam splitter (PBS) to produce orthogonal Pol_x and Pol_y channels observing at the "a" point, respectively, as seen in Fig. 3. An erbium-doped fiber amplifier (EDFA) is exploited to amplify the two signals and compensate the loss of WDM multiplexer behind the "b" point for downstream transmission in the CO. So, the observed output power of each wavelength is 7.5 dBm at the "b" point of Fig. 3. The 3-port optical circulator (OC) is employed to separate the downstream and upstream traffic in this setup. After 25 km SMF link, the dual-polarized downstream traffic is separated two wavelengths by the CPR. One will enter the 25G ONU directly and the other will launch into 10G ONU through 80 km SMF link. In fact, the polarization direction would rotate through a length of SMF transmission. Thus, a PC is applied at the Rx side to adjust the proper polarization status for passing and decoding signal. As seen in Fig. 3, the x- and y-POLs are used in the 25G ONU and 10G ONU to match the corresponding Pol_x and Pol_y wavelengths by adjusting the PC, respectively. Moreover, an optical pre-amplifier, which
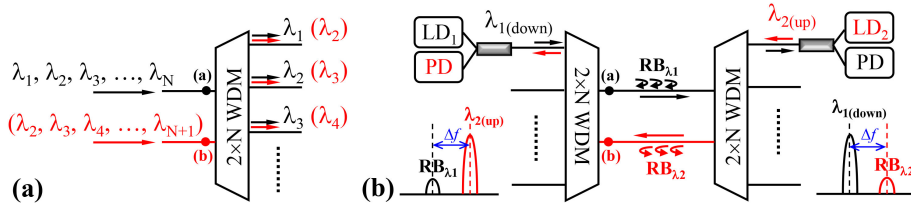
Fig. 2. (a) The diagram of periodic wavelength arrangement for $2 \times N$ WDM multiplexer. (b) The schematic of RB-induced noises of downstream and upstream ($RB_{\lambda 1}$ and $RB_{\lambda 2}$) in the presented PON system.
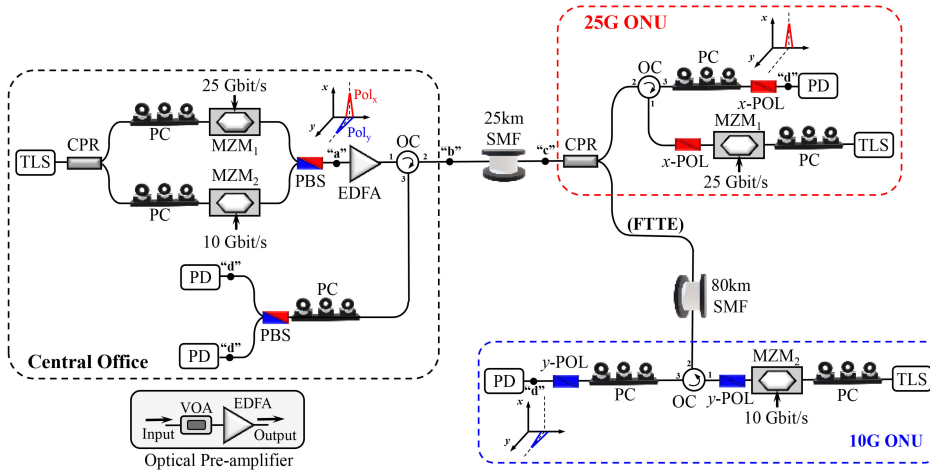

Fig. 3. Experimental setup of proposed PDM WDM-PON architecture with long-reach FTTE application for proof of concept.
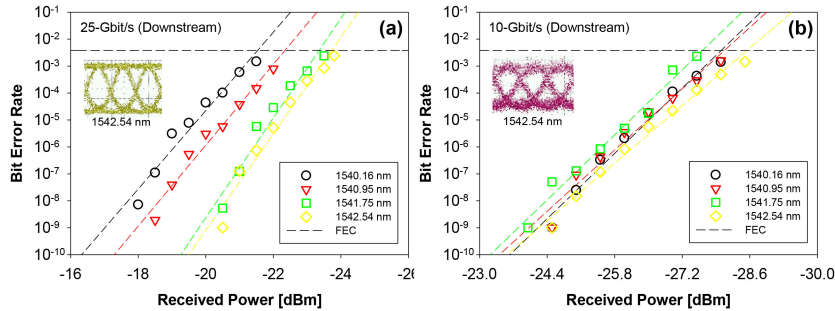

Fig. 4. Measured BER performances of (a) 25 and (b) 10 Gbit/s OOK downstream traffic after 25 and 105 km SMF connections, respectively, at the wavelengths of λ_1 to λ_4.

consists of a variable optical attenuator (VOA) and an EDFA, is placed at the "d" point to amplify and enhance the detected signal performance of downstream and upstream. The VOA is used to simulate the different received power of downstream signal for bit error rate (BER) measurement. As plotted in Fig. 3, we apply 25 and 10 Gbit/s OOK modulation with pattern length of $2^{31}-1$ on the 40 GHz MZM_1 and 10 GHz MZM_2 by using BER tester respectively, to generate dual-polarized downstream signals. This means that each wavelength can carry 35 Gbit/s downstream capacity for end user.

Figs. 4(a) and (b) display the observed BER measurements of 25 and 10 Gbit/s OOK downstream traffic through 25 and 105 km SMF connections, respectively, at the wavelengths of λ_1 to λ_4. The observed power sensitivities of four 25 Gbit/s OOK downstream traffic are $-21.5, -22.4, -23.4$ and -23.7 dBm,

respectively, after 25 km SMF transmission at the forward error correction (FEC) target (BER $\leq 3.8 \times 10^{-3}$), as shown in Fig. 4(a). Thus, the available power budgets of 29, 29.9, 30.9 and 31.2 dB can be obtained in the proposed PDM WDM-PON with FTTE architecture. When the downstream wavelength leaves the CO, the signal will pass through the 25 km SMF (5 dB), a CPR (3 dB), an OC (0.5 dB), a PC (1 dB) and a x-POL (1 dB) and then into the 40 GHz photodiode (PD) for decoding signal. Besides, according to the proposed network schemes of Fig. 1, one WDM multiplexer (6 dB) is behind the "b" point of Fig. 3, another is at the "c" point of Fig. 3. The total insertion loss of the presented access network of Fig. 3 is nearly 16.5 dB. Hence, based on the achieved power budget of each downstream channel, all the downstream signals can satisfy the FEC threshold for 25 Gbit/s short-reach fiber connection without dispersion compensation.
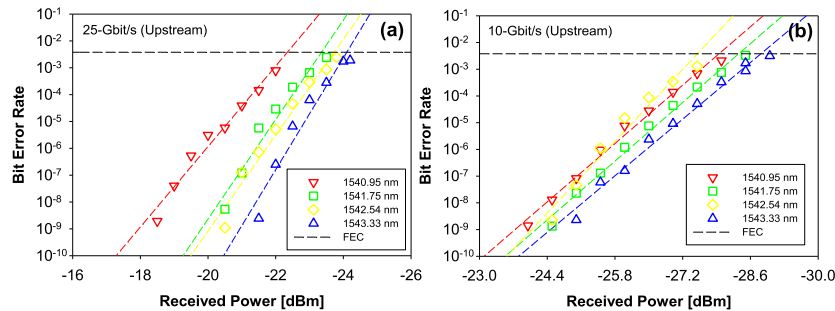
Fig. 5. Measured BER performances of (a) 25 and (b) 10 Gbit/s OOK upstream traffic after 25 and 105 km SMF connections, respectively, at the wavelengths of λ_2 to λ_5.

As plotted in Fig. 3, the total SMF transmission length is 105 km for each 10 Gbit/s OOK downstream signal via FTTE link. Fig. 4(b) displays the measured 10 Gbit/s OOK downstream performance of the same wavelengths after 105 km SMF transmission. We obtain that the detected power sensitivities of four downstream channels are –28.0, –28.1, –27.6 and –28.5 dBm without dispersion compensation, respectively, as seen in Fig. 4(b). Therefore, the four corresponding power budgets are 35.5, 35.6, 35.1 and 36 dB. Moreover, the 10 Gbit/s downstream traffic will experience 105 km SMF (21 dB), a WDM multiplexer (6 dB), a CPR (3 dB), an OC (0.5 dB), a PC (1 dB) and y-POL (1 dB) and then into the 10 GHz photodiode (PD). The total insertion loss of 32.5 dB is caused in the presented PON network. The results show that each 10 Gbit/s downstream channel can be less than FEC limit for receiving data. The insets of Figs. 4(a) and 4(b) are the measured eye diagrams of 25 and 10 Gbit/s OOK modulation at error free status, when the wavelength is set at 1542.54 nm for demonstration. The observed eyes are open and clear. In addition, in this experiment we do not exploit any dispersion compensation and the SMF transmission lengths of 10 and 25 Gbit/s OOK signals are 105 and 25 km, respectively. Hence, the measured diagram of 25 Gbit/s has a better eye-opening than that 10 Gbit/s, due to the effect of chromatic dispersion.

Then, we experiment the upstream signal performance from the 25G ONU and 10G ONU, respectively, according to the setup of Fig. 3. The wavelengths of 1540.95 (λ_2), 1541.75 (λ_3), and 1542.54 nm (λ_4) and 1543.33 nm (λ_5) are selected for measurement. The upstream wavelengths of λ_2 to λ_5 could pass through the "b" connected port of $2 \times N$ WDM multiplexer, as seen in Fig. 1. In the 25G and 10G ONUs, we utilize the POL_x and POL_y to generate the 25 Gbit/s Pol_x- and 10 Gbit/s Pol_y-based upstream wavelengths, respectively, as seen in Fig. 3. After leaving the ONU, each upstream output power is nearly 7.5 dBm. The four 25 Gbit/s OOK upstream channels will experience an OC (0.5 dB), a CPR (3 dB), a length of 25 km SMF (5 dB), a PC (1 dB) and a PBS (3 dB), and then into the corresponding PD for demodulation. These components could induce a total insertion loss of 12.5 dB. Fig. 5(a) present the measured BER characteristics of four 25 Gbit/s OOK upstream signals after 25 km SMF connection. To be below the FEC threshold, the four power sensitivities of –22.3, –23.4, –23.7 and –24.1 dBm are achieved, respectively. The corresponding
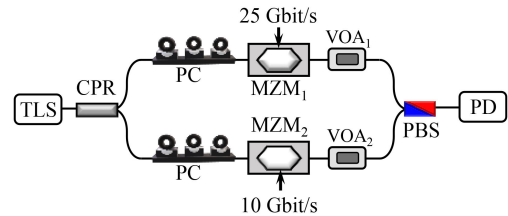
power budgets are between 29.8 and 31.5 dB among the four wavelengths.

As schemed in Fig. 3, the 10 Gbit/s OOK upstream channels pass through 105 km SMF (21 dB) transmission. Thus, the total insertion would become 28.5 dB. Fig. 5(b) exhibit the BER measurements of four 10 Gbit/s upstream traffic through 105 km SMF link. We observe that the four power sensitivities are –27.9, –28.3, –27.5 and –28.8 dBm at the FEC limit, respectively. Therefore, the allowable range of power budget is between 35 and 36.3 dB. In addition, according to the obtained results of Figs. 4 and 5, the total insertion loss could not affect the 25 and 10 Gbit/s downstream and upstream signal performances.

Normally, to achieve data security in success network, the advanced optical signal processing has demonstrated, such as using the optical CDMA, OFDM, and phase extraction scheme [24]–[26]. In the investigation, the dual-polarized 25 and 10 Gbit/s OOK modulations are mixed for delivering downstream and upstream. So, two various overlapping OOK wavelengths will cause a chaotic signal sequence to produce data security before receiving and decoding. The unauthorized user maybe could occupy the two mixed dual-polarized signals. However, to the unauthorized person, the occupied data signal is a chaotic sequence and hard to decode. Besides, the unauthorized user also needs to know whether there is a dual-polarization technology in such PON. Moreover, the angle between the two orthogonal polarizations on the x-axis is not limited to 0°, it can also be set at 30°, 45° or other. This will also increase the difficulty of decoding data in the physical layer.

In previous study [27], the long-reach PONs could integrate access and metro sections and simplify network architecture for reducing cost. And the WDM can be used to fully utilize the fiber bandwidth. The proposed PDM WDM-PON architecture

Fig. 6. Experimental setup of hybrid 25 and 10 Gbit/s for signal security measurement.
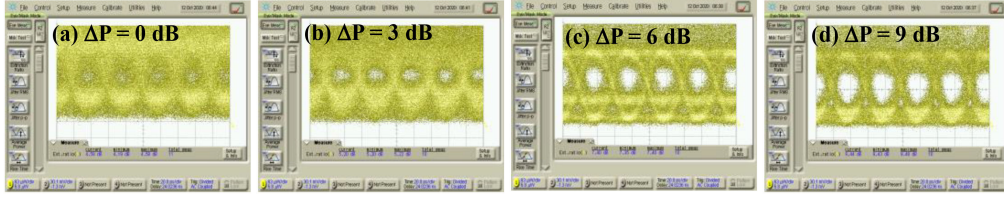
Fig. 7. Observed eye diagram of 25 Gbit/s OOK signal when a 10 Gbit/s is blended at the power differences of (a) 0, (b) 3, (c) 6 and (d) 9 dB, respectively.
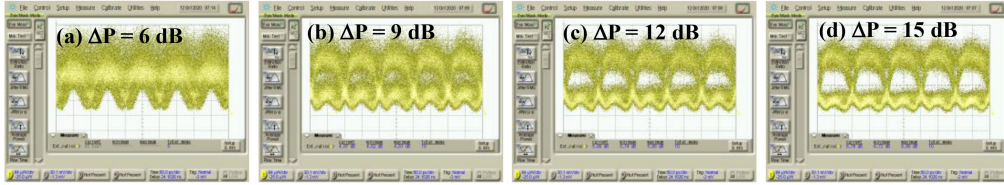

Fig. 8. Observed eye diagram of 10 Gbit/s OOK signal when a 25 Gbit/s is blended at the power differences of (a) 6, (b) 9, (c) 12 and (d) 15 dB, respectively.

combines the 25 km standard-reach and 105 km long-reach PONs via dual-polarized single wavelength to provide 25 and 10 Gbit/s OOK downstream and upstream traffics simultaneously. Therefore, the presented WDM access network can reduce the light sources via dual-polarized method and enhance the signal capacity to each ONU from standard to long-reach fiber connections.

To realize the interference effect of dual-polarized downstream for data security in physical layer, the 25 Gbit/s Pol_x-based and 10 Gbit/s Pol_x-based OOK wavelengths are applied in an experiment setup of Fig. 6 for proof of concept. As seen in Fig. 3, the optical devices of PBS and CPR may be caused different insertion loss at certain connected port after using for a period or affected by man-made. Therefore, the last experiment is proposed to explore the effect of different received powers of dual-polarized signals on BER performance. We use two VOAs (VOA_1 and VOA_2) to adjust the different output powers (P_{25G} and P_{10G}) for measuring the corresponding eye diagram, when two various modulation signals are blended. Originally, the two modulated signals are set at –3 dBm under error free status. First, we execute the eye observation of 25 Gbit/s OOK signal by using an oscilloscope. Here, 10 Gbit/s OOK wavelength would become an interference signal. In the demonstration, the P_{25G} is fixed and the P_{10G} is reduced gradually to observe the change of 25 Gbit/s eye distribution. Figs. 7(a) to (d) show the measured eye diagrams when the power difference ($\Delta P = P_{25G} - P_{10G}$) is 0, 3, 6 and 9 dB, respectively. The observed eye diagram is unclean when the ΔP is 0 and 3 dB, respectively. To attain and decode the original 25 Gbit/s signal information when the ΔP is gradually greater than 6 dB to open the eye for decoding, as shown in Figs. 7(c) and (d).

To observe the 10 Gbit/s OOK eye performance, the P_{10G} is fixed and the P_{25G} is adjusted to decrease slowly in the measurement. The measured 10 Gbit/s OOK eyes are illustrated in Fig. 8(a) to (d), respectively, when the power difference ΔP ($P_{10G} - P_{25G}$) is 6, 9, 12 and 15 dB. Here, as the ΔP is larger than 6 dB, the corresponding eye could not be observed. When the ΔP reduce to 6 and 9 dB, the observed eyes are also not open

and clean, as seen in Figs. 8(a) and (b). To open the eye for signal demodulation, the ΔP must be larger than 12 dB, as illustrated in Figs. 8(c) and (d). According to the measured results of Figs. 7 and 8, 10 Git/s signal will be affected more severely than 25 Gbit/s signal, when the ΔP at the same status. This is because the modulation sequence of 25 Gbit/s OOK format is greater than that of 10 Gbit/s signal. Therefore, the 10 Gbit/s modulation format become worse when the 25 Gbit/s signal is mixed. In the proposed PON network, the two dual-polarized downstream signals would have similar power. For the unauthorized user, the detected downstream wavelength only shows jamming signal sequence. Therefore, the two combined PDM signals could not be decoded for downstream data security, due to the optical interference.

III. CONCLUSION

We proposed and investigated a symmetric PDM WDM-PON network with FTTE architecture for long-reach data access. Here, each WDM downstream wavelength could produce the Pol_x- and Pol_y-based channels to carry 25 and 10 Gbit/s OOK traffic for 25 km short-reach and 105 km long-reach fiber transmissions without dispersion compensation, respectively. Based on the periodic output feature of $2 \times N$ WDM multiplexer in the proposed PON architecture, the RB beat noise also could be avoided. To demonstrate and perform the bidirectional data rate traffic, four wavelengths of λ_1 to λ_4 and λ_2 to λ_5 were applied to serve as the downstream and upstream wavelengths, respectively. In the measured results, the minimal power budget of 25 and 10 Gbit/s downstream and upstream signals were 29 and 35.1 dB and 29.8 and 31.5 dB, respectively, within the FEC threshold. All obtained power budgets were greater than the total insertion loss caused by the presented PON network. Hence, the bidirectional data traffic could be achieved in the PON system without the need of optical amplification. Moreover, the downstream wavelength would produce jamming sequence signal to secure the information owing to the two combined signals of 25 and 10 Gbit/s data rates, when the unauthorized user

occupied unlawfully. As a result, the presented PDM WDM-PON architecture not only provided symmetric 35 Gbit/s downstream and upstream transmissions by employing dual-polarized wavelength, but also achieved the RB noise mitigation and produced the data security and protection.

REFERENCES

[1] K.-M. Choi, S.-M. Lee, M.-H. Kim, and C.-H. Lee, "An efficient evolution method from TDM-PON to next-generation PON," *IEEE Photon. Technol. Lett.*, vol. 19, no. 9, pp. 647–649, May 2007.

[2] H.-Y. Wang, C.-H. Cheng, C.-T. Tsai, Y.-C. Chi, and G.-R. Lin, "Multicolor laser diode heterodyned 28-GHz millimeter-wave carrier encoded with DMT for 5G wireless mobile networks," *IEEE Access*, vol. 7, pp. 122697–122706, Aug. 2019.

[3] S. Shen, Y.-W. Chen, Q. Zhou, J. Finkelstein, and G.-K. Chang, "Demonstration of pattern division multiple access with message passing algorithm for multi-channel mmWave uplinks via RoF mobile fronthaul," *J. Lightw. Technol.*, vol. 38, no. 20, pp. 5908–5915, 2020.

[4] C.-H. Yeh, J.-R. Chen, W.-Y. You, W.-P. Lin, and C.-W. Chow, "Rayleigh backscattering noise alleviation in long-reach ring-based WDM access communication," *IEEE Access*, vol. 8, pp. 105065–105070, Jun. 2020.

[5] X. Wu, D. Zhang, Z. Ye, H. Lin, and X. Liu, "Real-time demonstration of 20 × 25 Gb/s WDM-PON for 5G fronthual with embedded OAM and type-B protection," in *Proc. 2019 24th OptoElectronics Commun. Conf. (OECC) and 2019 Int. Conf. Photonics Switching Comput. (PSC)*, 2019, paper TuA3-2.

[6] J. Zhang, Y. Xiao, D. Song, L. Bai, and Y. Ji, "Joint wavelength, antenna, and radio resource block allocation for massive MIMO enabled beamforming in a TWDM-PON based fronthaul," *J. Lightw. Technol.*, vol. 37, no. 4, pp. 1396–1407, 2019.

[7] C.-W. Chow and C.-H. Yeh, "Using downstream DPSK and upstream wavelength-shifted ASK for rayleigh backscattering mitigation in TDM-PON to WDM-PON migration scheme," *IEEE Photon. J.*, vol. 5, no. 2, Apr. 2013, Art. no. 7900407.

[8] Y. Luo *et al.*, "Time- and wavelength-division multiplexed passive optical network (TWDM-PON) for next-generation PON stage 2 (NG-PON2)," *J. Lightw. Technol.*, vol. 31, no. 4, pp. 587–593, 2013.

[9] X. Chen and J. Yao, "Wavelength reuse in a symmetrical radio over WDM-PON based on polarization multiplexing and coherent detection," *J. Lightw. Technol.*, vol. 34, no. 4, pp. 1150–1157, 2016.

[10] H.-D. Jung, N.-C. Tran, C. Okonkwo, E. Tangdiongga, and T. Koonen, "10Gb/s bi-directional symmetric WDM-PON system based on POLMUX technique with polarization insensitive oNU," in *Proc. Optical Fiber Commun. Conf.*, 2010, paper JThA27.

[11] C. Liu *et al.*, "Design and simulation of OFDM-PON combined with polarization multiplexing and coherent detection," in *Proc. IEEE 2nd Int. Conf. Electron. Commun. Eng.*, Dec. 2019, pp. 79–83.

[12] G. C. Mandal, R. Mukherjee, B. Das, and A. S. Patra, "Next-generation bidirectional triple-play services using RSOA based WDM radio on free-space optics PON," *Opt. Commun.*, vol. 411, pp. 138–142, 2018.

[13] G. C. Mandal, R. Mukherjee, B. Das, and A. S. Patra, "Bidirectional and simultaneous transmission of baseband and wireless signals over RSOA based WDM radio-over-fiber passive optical network using incoherent light injection technique," *Int. J. Electron. Common.*, vol. 80, pp. 193–198, 2017.

[14] H.-W. Wu, C.-Y. Li, H.-H. Lu, Q.-P. Huang, S.-C. Tu, and Y.-C. Huang, "A PDM-based 128-Gb/s PAM4 fibre-FSO convergent system with OBPFs for polarisation de-multiplexing," *Sci. Rep.*, vol. 10, no. 1, 2020, Art. no. 1872.

[15] W.-S. Tsai, H.-H. Lu, Y.-C. Huang, S.-C. Tu, and Q.-P. Huang, "A PDM-based bi-directional fibre-FSO integration with two RSOAs scheme," *Sci. Rep.*, vol. 9, no. 1, 2019, Art. no. 8317.

[16] C.-W. Chow, C.-H. Yeh, L. Xu, and H.-K. Tsang, "Rayleigh backscattering mitigation using wavelength splitting for heterogeneous optical wired and wireless access," *IEEE Photon. Technol. Lett.*, vol. 2, no. 17, pp. 1294–1296, Sept. 2010.

[17] Y.-T. Hsueh, M.-F. Huang, S.-H. Fan, and G.-K. Chang, "A novel lightwave centralized bidirectional hybrid access network: Seamless integration of RoF with WDM-OFDM-PON," *IEEE Photon. Technol. Lett.*, vol. 23, no. 15, pp. 1085–1087, Aug. 2011.

[18] M. Patel, A. Darji, D. Patel, and U. Dalal, "Mitigation of RB noise in bidirectional fiber transmission systems based on different OFDM SSB techniques," *Opt. Commun.*, vol. 426, pp. 273–277, 2018.

[19] G. Berrettini *et al.*, "Colorless WDM-PON architecture for rayleigh backscattering and path-loss degradation mitigation," *IEEE Photon. Technol. Lett.*, vol. 21, no. 7, pp. 453–455, 2009.

[20] C.-H. Yeh and C.-W. Chow, "Signal remodulation ring WDM passive optical network with rayleigh backscattering interferometric noise mitigation," *IEEE Commun. Lett.*, vol. 15, no. 10, pp. 1114–1116, 2011.

[21] S.-C. Lin, S.-L. Lee, H.-H. Lin, G. Keiser, and R. J. Ram, "Cross-seeding schemes for WDM-based next-generation optical access networks," *J. Lightw. Technol.*, vol. 29, no. 24, pp. 3727–3736, Dec. 2011.

[22] Z. Li, Y. Dong, Y. Wang, and C. Lu, "A novel PSK-Manchester modulation format in 10-Gb/s passive optical network system with high tolerance to beat interference noise," *IEEE Photon. Technol. Lett.*, vol. 17, pp. 1118–1120, May 2005.

[23] P. Mandal, K. Mallick, B. Dutta, B. Kuiri, S. Santra, and A. S. Patra, "Mitigation of rayleigh backscattering in RoF-WDM-PON employing self coherent detection and bi-directional cross wavelength technique," *Opt. Quantum Electron.*, vol. 53, no. 2, 2021, Art. no. 77.

[24] W. Chen, "Optical data security system using phase extraction scheme via single-pixel detection," *IEEE Photon. J.*, vol. 8, no. 1, Feb. 2016, Art. no. 7801507.

[25] M. P. Fok, K. Kravtsov, Y. Deng, Z. Wang, and P. R. Prucnal, "Providing network security with optical signal processing," in *Proc. IEEE PhotonicsGlobal@Singap.*, pp. 1–4, Dec. 2008.

[26] X. Yang, A. Sultan, A. Hajomer, L. Zhang, and W. Hu, "Physical-layer OFDM data encryption using chaotic QAM mapping," in *Proc. ICTON*, 2019, paper Th.C1.4.

[27] C.-H. Yeh, C.-W. Chow, Y.-F. Wu, J.-Y. Sung, Y.-L. Liu, and C.-L. Pan, "Performance of long-reach passive access networks using injection-locked fabry-perot laser diodes with finite front-facet reflectivities," *J. Lightw. Technol.*, vol. 31, no. 12, pp. 1929–1934, 2013.